DEVELOPING A VISIBLE CHANNEL CALIBRATION ALGORITHM FOR COMS OVER OCEAN AND DESERT TARGETS

B.J. Sohn, Hyoung-Wook Chun, and Jung-Geun Kim

School of Earth and Environmental Sciences, Seoul National University, Seoul, 151-747, Korea : sohn@snu.ac.kr

The Korean Geostationary satellite (COMS) to fly in year 2009 will carry a meteorological sensor from which visible channel measurements will be available. We developed a method utilizing satellite-derived BRDFs for the solar channel calibration over the bright desert area. The 6S model has been incorporated to account for directional effects of the surface using MODIS-derived BRDF parameters within the spectral interval in interest. Simulated radiances over the desert targets were compared with MODIS and SeaWiFS measured spectral radiances in order to examine the feasibility of the developed calibration algorithm. We also simulated TOA radiance over ocean targets to verify the consistency and reliability of the result. It was shown that simulated 16-day averaged radiances are in good agreement with the satellite-measured radiances within about ±5% uncertainty range for the year 2005, suggesting that the developed algorithm can be used for calibrating the COMS visible channel within about 5% uncertainty level.

KEY WORDS: Solar channel calibration, BRDF, COMS, MODIS, SeaWiFS

1. INTRODUCTION

Communication Ocean Meteorological Satellite (COMS) planned to launch in 2009 will be the first Korean geostationary satellite. The onboard Meteorological Imager (MI) will measure the reflected solar radiation within a spectral band (550 ~ 800 nm) as well as emitted infrared radiation at 4 spectral bands. Absolute calibration of the radiometer is prerequisite for the accurate measurements of various atmospheric and surface parameters as well as monitoring the sensor drift. However, because no in-flight calibration device will be available for the solar channel, any alternate way is necessary for the sensor calibration.

In this study we develop a method of utilizing satellite-derived BRDF for calculating the TOA radiance which then will be used for the COMS solar channel calibration. Bright desert targets are chosen because the atmospheric contribution to the TOA radiance is fractionally smaller, compared to the surface contribution over the bright surface. Spatial and temporal variations of MODIS-derived nadir bidirectional reflectance distribution function (BRDF) and NDVI are examined over the Australian Simpson desert in order to select the bright surface area. Seasonally varying BRDFs over the selected targets are used as inputs to the 6S radiative transfer model to simulate visible channel radiances. Computed radiances are then compared with MODIS and SeaWiFS radiances observed to evaluate the uncertainty level of the developed calibration algorithm. We also simulated TOA radiance over ocean targets to verify the consistency and reliability of the result.

2. METHODOLOGY

2.1 Surface characterization

Since surface reflectance varies with positions of sun and satellite, information on the bidirectional reflectance distribution function (BRDF) is necessary for accurate calculation of the TOA radiance. In this study, BRDF information derived from MODIS/TERRA measurements is used, which is from the composite of all available cloud-free, atmospherically corrected, spectral surface reflectance observations over a 16-day period with a semi-empirical, kernel-driven BRDF model (Lucht et al., 2000). The theoretical basis of this kernel-driven BRDF model is that the land surface reflectance can be modeled as a sum of three kernels representing basic scattering types: (1) isotropic scattering, (2) radiative transfer-type volumetric scattering from horizontally homogeneous leaf canopies, and (3) geometric-optical surface scattering from scenes containing 3-D objects that cast shadows and are mutually obscured from view at off-nadir angles (Lucht et al., 2000).

The black and white sky albedos are used in this study. The black sky albedo is the reflectance from direct illumination source taking places over the 2 solid angle. This albedo is derived from integration of BRDF over the hemisphere (2 solid angle), so it is a function of solar zenith angle. The black sky albedo at the solar zenith angle of 10 is used for the calculation of the spectral surface reflectance (see 2.3 section). Because the white sky albedo is the reflectance in all directions from isotropic diffuse source, it can be obtained by integrating black sky albedo over illumination hemisphere and therefore is independent of angles. The white sky albedo is used as input to the radiative transfer model, along with BRDF.

2.2 Target selection

We use the brightness, spatial uniformity, temporal stability and spectral stability as criteria for selecting bright targets (Mitchell et al. 1997). The brightness of the target is important because the impact of uncertainties on measurement and characterization leads to the relative error inversely related to the brightness. The nadir BRDF (N. BRDF) is used for the brightness test. Spatial uniformity is also important because unavoidable registration error introduces significant uncertainty into the calibration method when the surface is not spatially uniform. Cosnefroy et al. (1996) computed the coefficient of variation (CV) which was defined by the ratio of normalized standard deviation to the mean of normalized TOA reflectance on a moving 41 x 41 pixel window in the METEOSAT-4 image. In this study, CV of N. BRDF is calculated at a 5 x 5 grid (about 20 x 20 km) window. Temporal stability is considered important for the sensor drift monitoring whereas spatial homogeneity is important element for the target selection. The NDVI is used for the spectral stability check at 11 potential targets given in Fig. 1. The potential targets (marked by gray circles in Fig. 1) are chosen when N. BRDF > 0.2, CV < 0.06, temporal standard deviation < 0.06, and NDVI < 0.2.

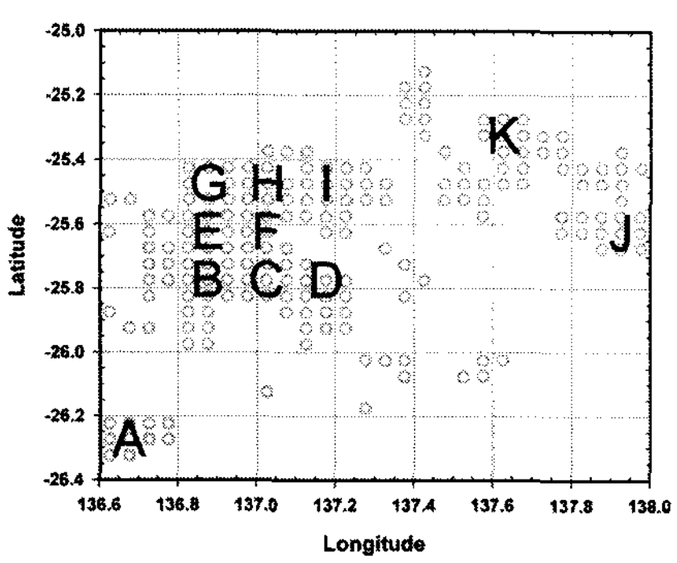

Figure 1. The location of 11 selected targets (A - K). The gray circles represent targets satisfying the target criteria.

2.3 Conversion of narrow band BRDF parameters to broad band parameters

Considering that COMS/MI solar channel will measure radiance over the broad band from 550 nm up to 800 nm, the MODIS BRDF parameters in seven bands are to be interpolated into the predefined wavelengths. The proposed method is based on the comparison of the black-sky albedo estimated at each MODIS band $\bar{\alpha}_{MO}(\mathbf{band, target, time})$ with the surface spectra from the ASTER spectral library (http://speclib.jpl.nasa.gov). The ASTER spectral library provides the spectral black sky-albedo at a 10° solar zenith angle $\alpha_{AS}(\lambda, \mathbf{type})$ from 400 nm up to 14000 nm for 41 surface types. The $\alpha_{AS}(\lambda, \mathbf{type})$ is converted into the spectral albedos at seven MODIS bands $\bar{\alpha}_{AS}(\mathbf{band, type})$ by applying MODIS response functions to $\alpha_{AS}(\lambda, \mathbf{type})$. Linear regression equation is obtained by relating $\bar{\alpha}_{MO}(\mathbf{band, target, time})$ to $\bar{\alpha}_{AS}(\mathbf{band, type})$. The surface type is selected at each target when the regression coefficient is largest. Then the spectral black sky albedo $\alpha(\lambda, \mathbf{target, time})$ is estimated from $\alpha_{AS}(\lambda, \mathbf{type})$ by applying the regression equation of the chosen soil type. Assuming the spectral variation of black-sky albedo $\partial\alpha/\partial\lambda$ is equal to that in BRDF parameters, MODIS BRDF parameters at seven bands are interpolated to wavelength band in interest using the spectral variation of BRDF parameters.

2.4 TOA radiance simulation over desert target

The TOA radiance is simulated using the 6S radiative transfer model (Vermote et al. 1997) for the given surface and atmospheric conditions. The spectral BRDF and albedo used for the specification of surface property are derived by interpolating spectral BRDF parameters at 7 MODIS bands into ones at each 2.5 nm between 450-900 nm. Because the atmospheric contribution to the TOA radiance is much weaker than the surface contribution over the bright desert, the atmospheric conditions are specified with climatological values, i.e.: total precipitable water of 2.0 g/cm^2, total ozone of 0.31 cm-ATM, and aerosol optical thickness at 500 nm of 0.1 representing the continental aerosol model. The model simulated TOA radiances over the Target B are compared with MODIS observed radiances for the year 2005.

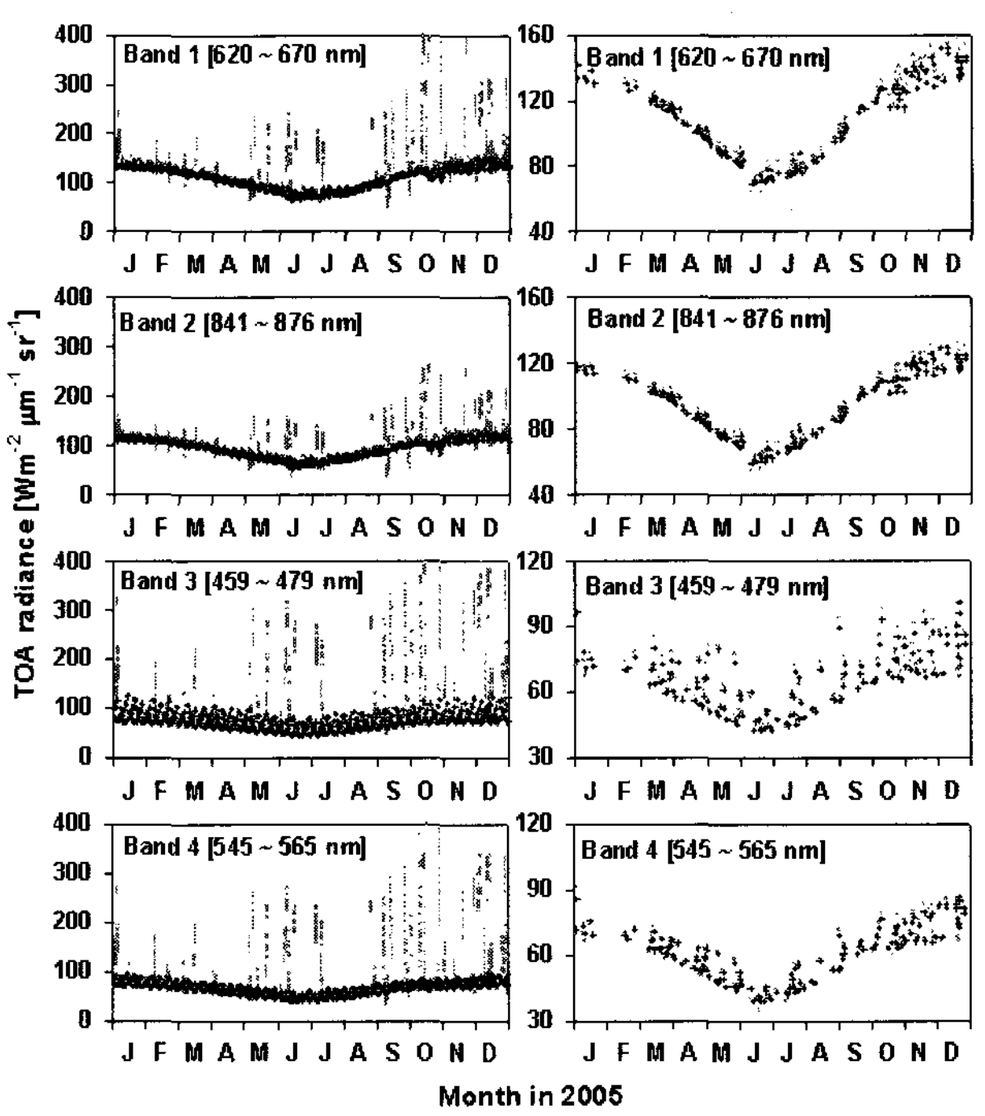

Figure. 2. Comparison of calculated radiances at all pixels in Target B with the observed values in year 2005. The black crosshair represents the MODIS-observed radiance whereas the gray dot represents the calculated radiance. The left and right panels are before the cloud screening and after the cloud screening, respectively.

Removing the contaminated scenes due to, for example, the presence of sand storms, broken clouds, and cloud shadows, a specific filtering mechanism similar to Govaerts et al (1998) has been developed. The mean value $\overline{\mathbf{R}}(\mathbf{t})$ and the corresponding standard deviation σ are estimated with two step procedures of rejecting extreme pixel values. First, $\overline{\mathbf{R}}(\mathbf{t})$ is obtained by taking average of values at all pixels. Then pixels showing radiance deviations larger than one σ are rejected and mean values are calculated from remaining pixel values. Corresponding observation range $\mathbf{r_d}$ is estimated by taking the difference between observed maximum and minimum. Furthermore, $\mathbf{R'(t)-\overline{R}(t)}$ is assumed to show a Gaussian distribution, in which their mean and standard deviation are defined by μ_d , σ_d , respectively. Finally pixel is assumed to be clear if $\left|(\mathbf{R'(t)-\overline{R}(t)})-\mu_d\right| \le \sigma_d$ and $\mathbf{r_d} \le 2\sigma_d$. Results obtained after completing the clearing procedures are compared with ones without cloud screening -- see Fig. 2.

2.5 TOA radiance simulation over ocean target

We also simulated TOA radiance over ocean targets to verify the consistency and reliability of the result. Ocean targets are chosen because the surface reflectance is easily determined and homogeneous dark target. In clear ocean, the surface reflectance is essentially determined by wind speed. But the TOA radiance over ocean targets is very sensitive to the aerosol because the surface reflectance is too small. Therefore we simulated TOA radiances only aerosol optical thickness is less than 0.1. TOA radiances were simulated with geometric angles and sensor characteristics of the reference satellite, wind speed from NCEP, aerosol optical thickness from MODIS/Terra, pigment concentration from SeaWiFS, and ozone amount from OMI as inputs to the 6S radiative transfer model.

3. RESULT

As surface characteristics of the desert are assumed to be accurate and stable over the time, the main error sources are from the instrumental radiometric noise and uncertainties associated with inaccurate atmospheric parameters. The ratios of calculated radiance to observed value over the 16-day period at each target is averaged to reduce temporal random errors -- see Fig. 3 for the case of MODIS. Then ratio representing the target is obtained by taking an average of pixel-based ratios in the target under the assumption that the surface characterization errors are not correlated to each other -- see Fig. 4 for the MODIS case and Fig. 5 for the SeaWiFS case.

The temporally and spatially averaged ratios for MODIS (See Fig. 4) and SeaWiFS (See Fig. 5) show that the computed radiance errors are in 5 % uncertainty range except June. It is thought that the large uncertainties during June are due to inaccurate information on the surface BRDF drawn from MODIS measurements in that particular month. There seems to be no other reasons why this approach works well except June. However, it is possible to remove the unreliable BRDF information using quality flag provided with BRDF parameters. The 5 % uncertainty range obtained from both MODIS and SeaWiFS measurements suggests that the method we developed in this study may provide the calibration tool for the Korean COMS with the similar 5 % uncertainty range.

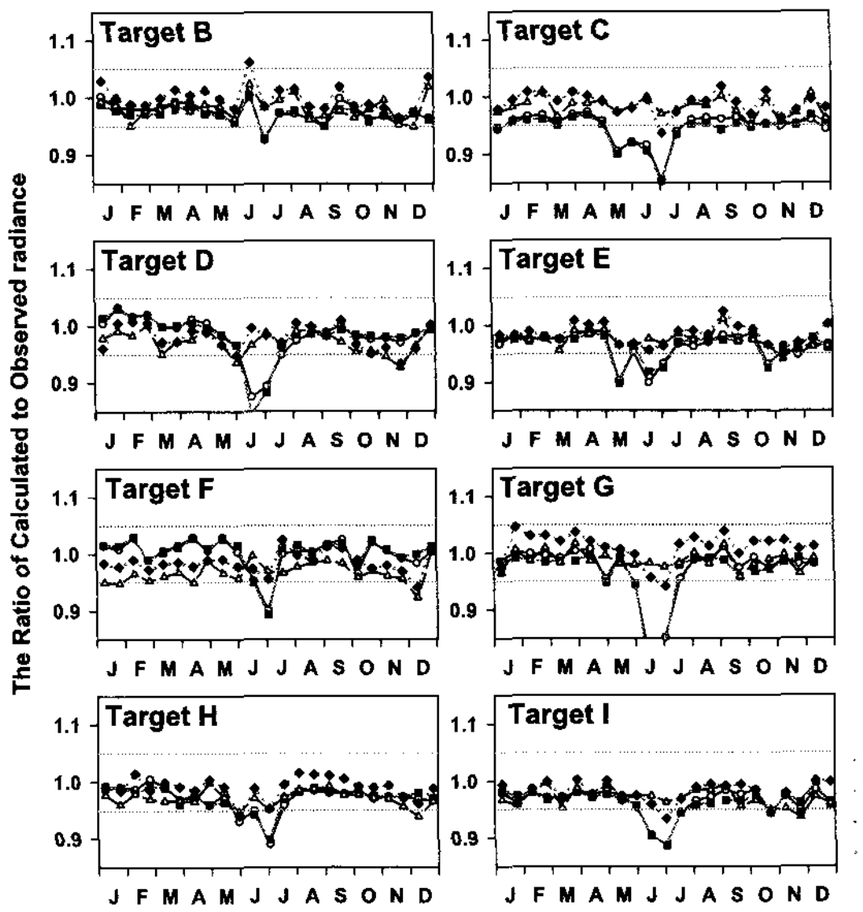

Fig. 3. The ratios of 6S model-calculated radiance to MODIS-observed value at each target: Band 1 (open circle), band 2 (solid square), band3 (open triangle), band 4 (solid diamond). Ratios were averaged for the 16 days.

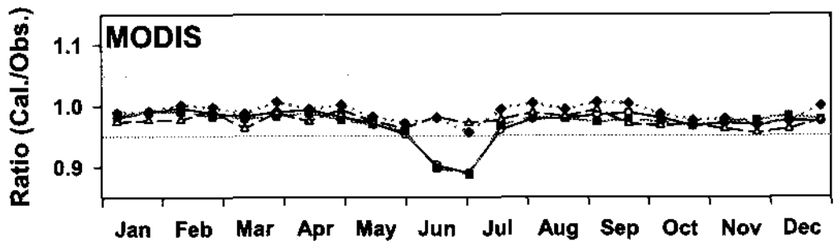

Fig. 4. The taget-averaged ratio of 6S model-calculated to the MODIS-observed value: Band 1 (open circle), band 2 (solid square), band3 (open triangle), band 4 (solid diamond).

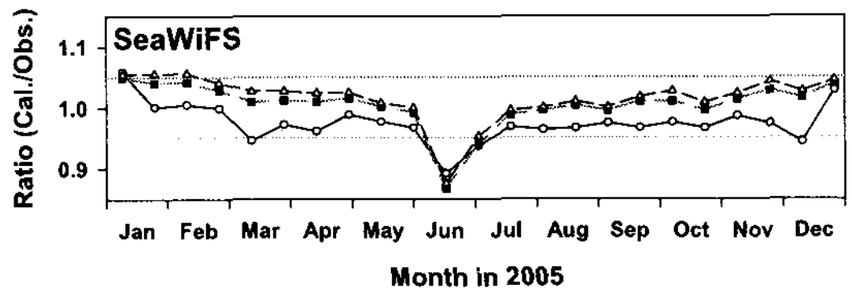

Fig. 5. Same as in Fig. 4 except for the SeaWiFS : Band 5 (open circle), band 6 (solid square), band7 (open triangle).

Table 1 shows the annual mean of spatially averaged ratio of calculated radiance to observed radiance at each MODIS and SeaWiFS bands. If we make the annual mean ratio, the relative bias between calculated and satellite-estimated values are within ±5% for all MODIS and SeaWiFS bands.

Table 1. The annual mean of spatial averaged ratio of calculated to observed radiances at each band.

Sensor	Band	Spectral range	Annual mean of Ratio
MODIS	Band 1	620 ~ 670 nm	0.971 ± 0.026
	Band 2	841 ~ 876 nm	0.970 ± 0.026
	Band 3	459 ~ 479 nm	0.975 ± 0.011
	Band 4	545 ~ 565 nm	0.988 ± 0.014
SeaWiFS	Band 5	545 ~ 565 nm	0.975 ± 0.032
	Band 6	660 ~ 680 nm	1.005 ± 0.038
	Band 7	745 ~ 785 nm	1.015 ± 0.038

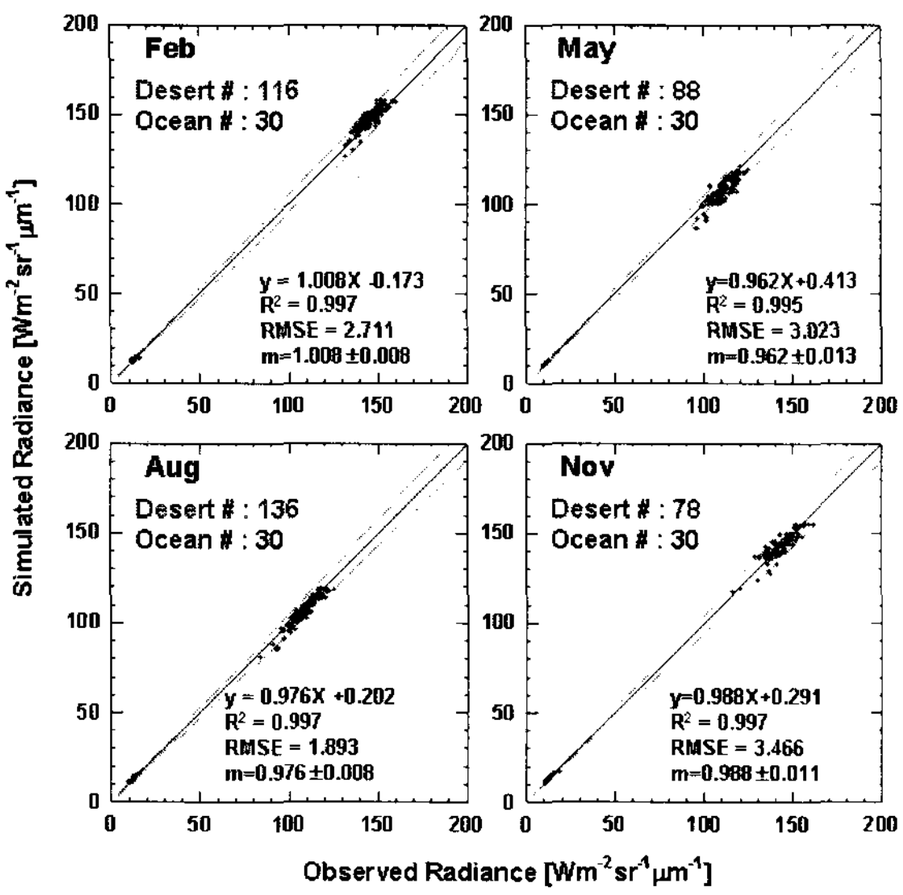

Fig. 6. Scatterplot of observe radiances against simulated radiance of SeaWiFS band 6 (670 nm) for Feb, May, Aug, and Nov over the desert targets and ocean targets.

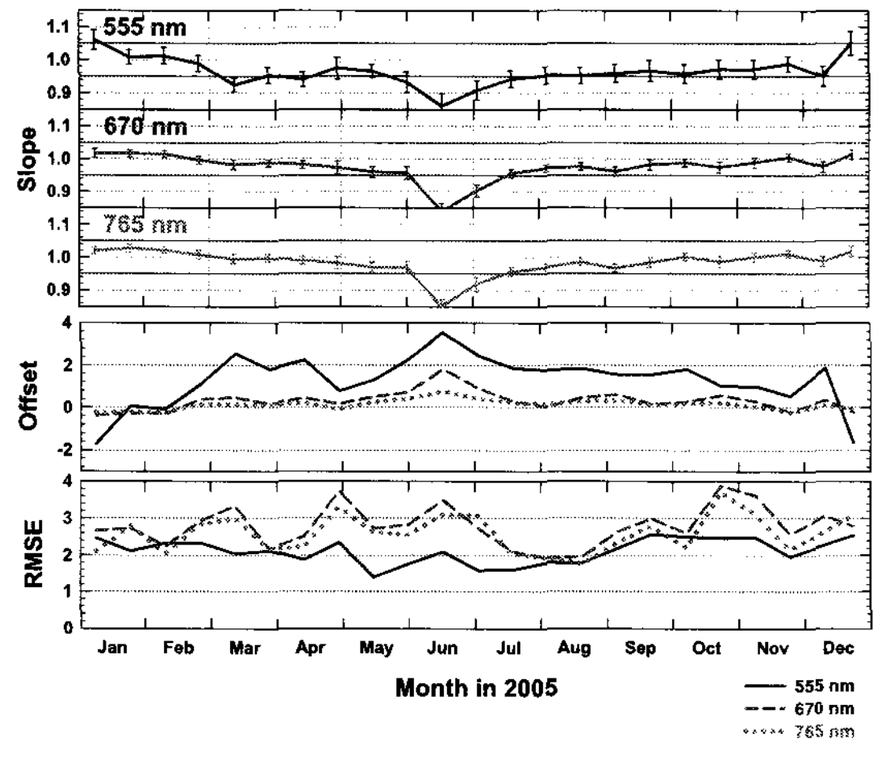

Fig. 7. Time series of slope, offset, and RMSE for SeaWiFS band 5, 6, 7 (555, 670, 765 nm)

We combined the radiance over ocean and desert target to evaluate the consistency -- see Fig. 6 for the case of SeaWiFS band 6. The dashed line is reference line represent 5 % error in Fig. 6. All results are located within 5 % error. Linear regression equation is obtained by relating observed radiance to simulated radiance every 16 day, and the time series of slope, offset, and RSME are showed in Fig. 7 for the case of SeaWiFS band 5, 6, 7. The slopes are in 1.0 ± 0.05 uncertainty range except June for all bands. The offsets are under 2.0 and RMSE are under 4.0. These values agree within 5 % relative error, because the radiances over desert target are larger than 100.

4. CONCLUSION

This paper describes a solar channel calibration algorithm for the Korean geostationary satellite COMS that will be launched in year 2009. Surface characterization was performed over the bright Australian desert by combining the MODIS BRDF parameter with the ASTER spectral database. Simulated radiances over the selected desert targets were compared with MODIS and SeaWiFS measured spectral radiances in order to examine the feasibility of the developed calibration method. Results suggest that the relative bias between calculated and satellite-estimated radiances are within ±5% uncertainly range when a large number of pixels are averaged over all selected desert targets, suggesting that the vicarious method developed in this study is suitable for calibrating the COMS visible senor within the suggested error range. Further efforts are still needed to improve the aerosol characterization.

ACKNOWLEDGEMENTS

This research has been supported by the Korean Geostationary Program (COMS) granted by the KMA, and by the BK21 Project of the Korean Government.

REFERENCES

Cosnefroy, H., M. Leroy, and X. Briottet, 1996. Selection and characterization of Saharan and Arabian desert sites for the calibration of optical satellite sensors. *Reomte Sensing Env.*, 58, pp. 101-114.

Govaerts, Y. M., B. Pinty, M. M. Verstraete, and J. Schmetz, 1998. Exploitation of angular signatures to calibrate geostationary satellite solar channels. *IGARSS'98 conference*, Seattle, USA, pp. 327-329.

Lucht, W., C. B. Schaaf, and A. H. Strahler, 2000. An Algorithm for the Retrieval of Albedo from Space Using Semiempirical BRDF Models. *IEEE Trans. Geosci. Remote Sensing*, 38, pp. 977-998.

Mitchell, R. M., D. M. O'Brien, M. Edwards, C. C. Elsum, and R. D. Graetz, 1997. Selection and Initial characterization of bright calibration site in the Strzelecki desert, South Australia. *Canadian J. Remote Sensing*, 23, pp. 342-353.

Vermote, E. F., D. Tanre, J. L. Deuze, M. Herman, and J. J. Morcrette, 1997. Second simulation of the satellite signal in the solar spectrum, 6S: An overview. *IEEE Trans. Geosci. Remote Sensing*, 35, pp. 675-686.